

Target Scattering Decomposition in Terms of Roll-Invariant Target Parameters

Ridha Touzi, *Member, IEEE*

Abstract—The Kennaugh–Huynen scattering matrix con-diagonalization is projected into the Pauli basis to derive a new scattering vector model for the representation of coherent target scattering. This model permits a polarization basis invariant representation of coherent target scattering in terms of five independent target parameters, the magnitude and phase of the symmetric scattering type introduced in this paper, and the maximum polarization parameters (orientation, helicity, and maximum return). The new scattering vector model served for the assessment of the Cloude–Pottier incoherent target decomposition. Whereas the Cloude–Pottier scattering type α and entropy H are roll invariant, β and the so-called target-phase parameters do depend on the target orientation angle for asymmetric scattering. The scattering vector model is then used as the basis for the development of new coherent and incoherent target decompositions in terms of unique and roll-invariant target parameters. It is shown that both the phase and magnitude of the symmetric scattering type should be used for an unambiguous description of symmetric target scattering. Target helicity is required for the assessment of the symmetry–asymmetry nature of target scattering. The symmetric scattering type phase is shown to be very promising for wetland classification in particular, using polarimetric Convair-580 synthetic aperture radar data collected over the Ramsar Mer Bleue wetland site to the east of Ottawa, ON, Canada.

Index Terms—Characteristic decomposition, coherency, coherent, diagonalization, eigenvalues, eigenvectors, entropy, incoherent, polarimetry, speckle, synthetic aperture radar (SAR), wetlands.

NOMENCLATURE AND ABBREVIATIONS

α - β model	Model introduced by Cloude and Pottier for parameterization of the coherency eigenvector.
CTD	Coherent target decomposition.
ICTD	Incoherent target decomposition.
SSCM	Symmetric scattering characterization method introduced by Touzi and Charbonneau for optimum characterization of the maximized target symmetric scattering.
LOS	Radar line of sight.
$[S]$	Scattering matrix.
μ_1 and μ_2	Scattering matrix coneigenvalues.
k	Target scattering vector introduced by Cloude.
α	Scattering type parameter introduced by Cloude and Pottier.

β	Orientation angle introduced by Cloude and Pottier.
α_s^c	Symmetric scattering type introduced in this paper as a complex entity.
α_s	Symmetric scattering type magnitude.
Φ_{α_s}	Symmetric scattering type phase.
ψ, τ_m, m	Kennaugh–Huynen maximum polarization parameters: orientation angle, helicity, and maximum amplitude.
$[T]$	Coherency matrix.
$\lambda_1, \lambda_2, \text{ and } \lambda_3$	Coherency eigenvalues.
λ_1	Eigenvalue of the dominant scattering.
λ_2	Eigenvalue of the second scattering.
λ_3	Eigenvalue of the third scattering.
H	Cloude coherency entropy.
α_{sg} and τ_g	Symmetric scattering type magnitude and helicity of the global scattering, respectively.

I. INTRODUCTION

THE OBJECTIVE of the incoherent target decomposition (ICTD) theory is to express the average scattering mechanism as the sum of independent elements in order to associate a physical mechanism with each component [1]–[4]. Target scattering decomposition permits the extraction of target characteristic information provided that the decomposition satisfies the general requirement of being robust under a change of wave polarization basis (i.e., roll invariant) [4]–[8]. Cloude–Pottier’s ICTD [1], [3], [7] is presently the most used method for decomposition of natural extended target scattering. The characteristic decomposition of the Hermitian target coherency matrix allowed Cloude and Pottier to derive key parameters, such as the scattering type α and the entropy H [1], [3], [9], which have become standard tools for target scattering classification and for geophysical parameter extraction from polarimetric synthetic aperture radar (SAR) data [4], [10]–[13].

To represent the coherent single scattering assigned to each target coherency eigenvector, Cloude and Pottier introduced the so-called α - β model [3], [9], which expresses the target scattering vector \vec{k} in terms of five parameters under reciprocity assumption, i.e.,

$$\vec{e}_T^{\alpha-\beta} = |\vec{e}_T| \cdot [\cos \alpha \cdot e^{j\Phi_1}, \sin \alpha \cos \beta e^{j\Phi_2}, \sin \alpha \sin \beta e^{j\Phi_3}]^T \quad (1)$$

where α is referred to as the scattering type, β is the target orientation angle, and Φ_i ($i = 1, 3$) are the target-phase angles [9], [14]. The most used parameter is α , which when combined with the Cloude entropy H , leads to the most popular approach

Manuscript received July 13, 2006; revised August 18, 2006. This work was supported in part by the Canadian Space Agency.

The author is with the Canada Centre for Remote Sensing, Natural Resources Canada, Ottawa, ON K1A 0Y7, Canada.

Digital Object Identifier 10.1109/TGRS.2006.886176

H/α for target scattering classification [3], [9]. β has been used for target tilt-angle measurement [15], [16]. In most of the applications that involve Cloude–Pottier target scattering decomposition, the target-phase angles Φ_i have been ignored, and their physical meaning is still not well understood.

Recently, some concerns have been raised concerning the Cloude–Pottier eigenvector parameterization. Lee *et al.* [16] have noted that β might not provide a pure measurement of the physical orientation angle (i.e., target tilt angle), and the right–left-like circular polarization (RR–LL) phase difference has been used (instead of β) to extract the orientation angle induced by the azimuthal slope from terrain surface scattering return [17]. Other concerns have been raised regarding the Cloude α 's scattering type ambiguities that occur for certain scatterers [18]. Corr and Rodrigues [18] pointed out the example of a helix and a dihedral, which are represented with the same α ($\alpha = 90^\circ$) and cannot be distinguished using the Cloude–Pottier H/α classification. To remove these scattering type ambiguities, Corr and Rodrigues [18] have applied Cloude–Pottier's ICTD in an alternative orthonormal basis formed with a sphere and a pair of left- and right-handed helices. They used the α – β model of (1) for parameterization of the three eigenvectors derived in the sphere–helices basis. The use of the alternative sphere–helix basis (instead of the Pauli matrix) leads to different β and Φ_i ($i = 1, 3$) parameters, and this permits solving for certain α scattering type ambiguities [18]. This is in agreement with one of our recent studies [19], in which we have shown that for an asymmetric target, β and the target-phase parameters Φ_i vary with the rotation of the incidence plane about the radar line of sight (LOS) and as such are not antenna polarization basis invariant.

In summary, even though the roll-invariant Cloude and Pottier H/α approach has been widely validated for scattering mechanism classification, investigation of the Cloude–Pottier α – β model's parameters, other than α , should be worthy for a more complete characterization of target scattering. These parameters should be roll invariant for the extraction of target characteristic information [5]–[8]. Therefore, there is a need for the assessment of the α – β model robustness under a change of wave polarization basis. This will be completed in this paper, and the problem raised by Corr and Rodrigues [18] regarding the scattering type ambiguities (related to the description of α) will also be investigated.

In the following, the Kennaugh–Huynen scattering matrix con-diagonalization [5], [6] is presented and projected into the Pauli basis to derive a new scattering vector model. A complex entity, the symmetric scattering type, is introduced for an unambiguous description of symmetric target scattering. The scattering vector model is then expressed in terms of five independent parameters for the representation of coherent target scattering; the Kennaugh–Huynen maximum polarization parameters (orientation, helicity, and maximum return [5], [6]), and the magnitude and phase of the symmetric scattering type. A comparative study between our scattering vector model and the Cloude–Pottier α – β model is covered in Section III. It is shown that the two models are identical for symmetric targets. For asymmetric targets, our scattering vector model remains roll invariant, whereas certain α – β model parameters vary with the orientation angle. In Section IV, the scattering vector model served as the basis for the development of a new CTD

that is shown to be unique and roll invariant. A unique and roll-invariant ICTD is also introduced for decomposition of partially coherent target scattering. Convair-580 polarimetric C-band SAR [20] data are used to validate the new ICTD in Section V. An illustration of our roll-invariant ICTD decomposition is presented, and a comparison with the Cloude–Pottier ICTD is conducted. The requirement for the use of both phase and magnitude of the symmetric scattering type for complete characterization of target scattering is demonstrated. The new symmetric scattering type phase is shown to be very promising for wetland classification in particular, using polarimetric SAR data collected over the RAMSAR Mer Bleue wetland in the east of Ottawa, ON, Canada.

II. NEW MODEL FOR CHARACTERIZATION OF COHERENT TARGET SCATTERING

A. Kennaugh–Huynen Con-Diagonalization

To fully exploit the information provided by coherent scattering, Kennaugh and Huynen [5], [6] have applied the characteristic decomposition on the scattering matrix $[S]$ using a nonconventional diagonalization procedure—the Takagi con-diagonalization [4], [21]. $[S]$ con-diagonalization leads to the so-called Kennaugh–Huynen con-diagonalization under the assumption of target reciprocity (i.e., $[S]$ symmetric) [4]–[6], [22]–[24], i.e.,

$$[S] = [R(\psi)][T(\tau_m)] \cdot [S_d] \cdot [T(\tau_m)][R(-\psi)] \quad (2)$$

where $[R(\psi)]$ is the transformation matrix for rotation by angle ψ , τ_m is the target helicity, and $[S_d]$ is a diagonal matrix with the $[S]$ coneigenvalues μ_1 and μ_2 as diagonal elements. $[R(\psi)]$ and $[T(\tau_m)]$ are given by

$$[R(\psi)] = \begin{bmatrix} \cos \psi & -\sin \psi \\ \sin \psi & \cos \psi \end{bmatrix} \quad (3)$$

and

$$[T(\tau_m)] = \begin{bmatrix} \cos \tau_m & -j \sin \tau_m \\ -j \sin \tau_m & \cos \tau_m \end{bmatrix}. \quad (4)$$

The $[S]$ con-diagonalization of (2) permits the characterization of each single scatterer with six independent parameters: ψ , τ_m , m , γ , ν , and ρ [5], [6], [25]. The maximum polarization parameters ψ , τ_m , and m are the orientation, the helicity, and the maximum amplitude return, respectively [5], [6]. These optimal polarization parameters are target characteristics since the maximum-power polarization parameters are target characteristics [5], [6]. ψ , which is the rotation angle applied to subtract the orientation angle effect on target scattering, provides an intrinsic measure of the target tilt angle [6]. The helicity τ_m is used to assess target symmetry. γ and ν are referred to as the characteristic and skip angle [6], respectively. ρ , which is the absolute phase of the target, is generally ignored, except for Pol-In SAR applications. The five parameters above, known as the Huynen parameters, were used by Huynen [25] as the basis of the so-called Huynen fork, which used to be the most popular method for characterization of coherent target scattering [4], [25]. However, some of Huynen's parameters

may not be unique because of the coneigenvalue phase ambiguity, as raised by E. Luneberg; “It should be pointed out that Huynen’s parameters are not unique and need to be reevaluated, in particular the skip angle, due to nonuniqueness of the coneigenvalue phases” [24]. The projection on the Pauli basis of the scattering matrix con-diagonalization, which is the basis of the new scattering vector model we are introducing here, permits circumventing the coneigenvalue phase ambiguity, as discussed in Section V-B.

B. Scattering Vector Model

The Kennaugh–Huynen con-diagonalization (2) is generally applied in the H – V linear polarization orthonormal basis. The Pauli basis offers a more convenient way for scattering representation [7], [26]. For a reciprocal target, the scattering matrix $[S]$ is symmetric, i.e., $S_{hv} = S_{vh}$, and target scattering is presented in terms of three orthogonal scattering mechanisms: a trihedral, a dihedral, and a 45° dihedral [3]. In order to derive the projection of the Kennaugh–Huynen con-diagonalization of (2) onto the Pauli basis, the matrix form of the Kennaugh–Huynen con-diagonalization model can be transformed into a vector form using the Kronecker product \otimes , i.e.,

$$\vec{S} = ([R(\psi)] \otimes [R(\psi)]) \cdot ([T(\tau_m)] \otimes [[T(\tau_m)])] \cdot \vec{S}_d \quad (5)$$

where $\vec{S} = (S_{hh}, S_{hv}, S_{vh}, S_{vv})^T$ and $\vec{S}_d = (\mu_1, 0, 0, \mu_2)^T$ are the vectorial forms of $[S]$ and $[S]_d$, respectively. V^T denotes the V transpose. Equation (5) can be symmetrized in the same way we did in [27] and then projected on the Pauli basis (S_a, S_b, S_c) given by

$$S_a = \begin{bmatrix} 1 & 0 \\ 0 & 1 \end{bmatrix} \quad (6)$$

$$S_b = \begin{bmatrix} 1 & 0 \\ 0 & -1 \end{bmatrix} \quad (7)$$

$$S_c = \begin{bmatrix} 0 & 1 \\ 1 & 0 \end{bmatrix}. \quad (8)$$

This leads to the following target scattering vector parametrization, which will be named the scattering vector model:

$$\vec{e}_T^{SV} = |\vec{e}_T|_m \cdot \exp^{j\Phi_s} \cdot \begin{bmatrix} 1 & 0 & 0 \\ 0 & \cos 2\psi & -\sin 2\psi \\ 0 & \sin 2\psi & \cos 2\psi \end{bmatrix} \cdot \vec{V}^{\text{orient-inv}} \quad (9)$$

where $|\vec{e}_T|_m = |\vec{e}_T^{SV}|/m$, and $\vec{V}^{\text{orient-inv}}$ is given as a function of target helicity τ_m and $[S]$ coneigenvalues μ_1 and μ_2 by

$$\vec{V}^{\text{orient-inv}} = m \cdot \begin{bmatrix} \frac{\mu_1 + \mu_2}{2} \cos 2\tau_m \\ \frac{\mu_1 - \mu_2}{2} \\ -j \frac{\mu_1 + \mu_2}{2} \sin 2\tau_m \end{bmatrix}. \quad (10)$$

The transformation matrix in (9) represents physically a rotation of the scatterer incidence plane about the radar LOS by the angle of orientation ψ . ψ is the orientation of the maximum polarization with respect to the horizontal polarization [25]. Elimination of ψ , or “desying” according to Huynen’s terminology [16], [25], consists of rotating the scattering

vector \vec{e}_T^{SV} about the LOS by the angle $-\psi$, and this leads to the orientation-invariant (i.e., roll-invariant) vector $\vec{V}^{\text{orient-inv}}$ of (10). The roll-invariant vector $\vec{V}^{\text{orient-inv}}$ is a function of the maximum polarization target intrinsic parameters τ_m and m and $[S]$ coneigenvalues μ_1 and μ_2 , which are polarization basis invariant.

C. Complex Entity for the Description of Symmetric Target Scattering: The Symmetric Scattering Type

Kennaugh [5], Huynen [6], Cameron *et al.* [28], Touzi and Charbonneau [29], and Touzi *et al.* [30] have attached great importance to a class of targets termed symmetric. A symmetric target is a target having an axis of symmetry in the plane orthogonal to the radar LOS direction [5], [6]. A symmetric target has zero helicity $\tau_m = 0$ [5], [6]. As a result, its scattering matrix can be diagonalized by a rigid rotation about the LOS, and its maximum polarization is a linear polarization that is either aligned with the target symmetry axis or orthogonal to it [5], [6]. In the following, we introduce a complex entity α_s^c , named the symmetric scattering type, for characterization of symmetric target scattering.

The polar coordinates α_s and Φ_{α_s} of α_s^c are defined as a function of the scattering matrix $[S]$ coneigenvalues μ_1 and μ_2 as follows:

$$\tan(\alpha_s) \cdot e^{j\Phi_{\alpha_s}} = \frac{\mu_1 - \mu_2}{\mu_1 + \mu_2}. \quad (11)$$

Like the Cloude α , the symmetric scattering type magnitude α_s is defined in the interval $0 \leq \alpha_s \leq \pi/2$ (i.e., $\cos \alpha_s \geq 0$ and $\sin \alpha_s \geq 0$). This leads to $-\pi/2 \leq \Phi_{\alpha_s} \leq \pi/2$. It can be shown that α_s is identical to the Cloude α for a symmetric target of low entropy, as discussed later in Section III.

For a symmetric target, the helicity τ_m is zero [5], [6], and the scattering vector model of (9) can be expressed as a function of α_s , Φ_{α_s} , and the orientation angle ψ as

$$\vec{e}_T^{SV} = m |\vec{e}_T|_m \cdot \exp^{j\Phi_s} \cdot \begin{bmatrix} 1 & 0 & 0 \\ 0 & \cos 2\psi & -\sin 2\psi \\ 0 & \sin 2\psi & \cos 2\psi \end{bmatrix} \cdot \begin{bmatrix} \cos \alpha_s \\ \sin \alpha_s e^{j\Phi_{\alpha_s}} \\ 0 \end{bmatrix} \quad (12)$$

where the phase Φ_s includes, in addition to the phase term of (9), the phase argument of $\mu_1 + \mu_2$. The symmetric target scattering matrix can be diagonalized by a rigid rotation about the LOS, as shown in (12). α_s is the angle of the symmetric scattering vector direction in the trihedral–dihedral (S_a, S_b) basis, whereas Φ_{α_s} is the phase difference between the vector components in the trihedral–dihedral basis. It is worth noting that the symmetric scattering type phase α_s and magnitude Φ_{α_s} , which are derived from the polarization basis invariant $[S]$ coneigenvalues, are also invariant under a change of antenna wave polarization basis. Notice also that α_s and Φ_{α_s} are identical to the SSCM parameters η and $\phi_{S_b} - \phi_{S_a}$ of [29] for a symmetric scatterer.

D. General Expression of the Scattering Vector Model for a Unique Characterization of Symmetric and Asymmetric Target Coherent Scattering

In the most general case, targets might be symmetric or asymmetric, and the scattering vector model of (12) can be extended to asymmetric targets as a function of target helicity τ_m

$$\vec{e}_T^{SV} = m |\vec{e}_T|_m \cdot \exp^{j\Phi_s} \cdot \begin{bmatrix} 1 & 0 & 0 \\ 0 & \cos 2\psi & -\sin 2\psi \\ 0 & \sin 2\psi & \cos 2\psi \end{bmatrix} \cdot \begin{bmatrix} \cos \alpha_s \cos 2\tau_m \\ \sin \alpha_s e^{j\Phi_{\alpha_s}} \\ -j \cos \alpha_s \sin 2\tau_m \end{bmatrix}. \quad (13)$$

Each coherent scatterer can be represented by the scattering vector model of (13) in terms of five independent parameters: the target orientation ψ and the four roll-invariant parameters α_s , Φ_{α_s} , τ_m , and m . The Φ_s of (13) can be ignored for non-interferometric applications. The maximum polarization is characterized with the orientation angle ψ and the ellipticity angle τ_m , where $-\pi/2 \leq \psi \leq \pi/2$ and $-\pi/4 \leq \tau_m \leq \pi/4$.

Huynen [25] has pointed out the existence of an orientation ambiguity related to the Kennaugh–Huynen diagonalization of (2). If ψ is the solution of (2), then $\psi \pm \pi/2$ are also solutions of (2) [25]. It can be shown that a similar ambiguity occurs with the scattering vector model's ψ angle, and the following relationship can be derived using (13):

$$\vec{e}_T^{SV}(\Phi_s, \psi, \tau_m, m, \alpha_s, \Phi_{\alpha_s}) = \vec{e}_T^{SV}(-\Phi_s, \psi \pm \pi/2, -\tau_m, m, \alpha_s, -\Phi_{\alpha_s}). \quad (14)$$

To remove the aforementioned ambiguity, the range of ψ is restricted to the interval $[-\pi/4, \pi/4]$ using (14), and the target tilt angle is measured modulo $\pi/2$.

It is worth noting that the transformation in (13) is unitary and preserves the length of the polarization basis invariant vector \vec{S}_d of (5). The latter one, which is equal [up to a multiplicative term (0.5)] to the rotation-invariant Grave matrix trace $|\mu_1|^2 + |\mu_2|^2$, corresponds to the total power scattered by the target, i.e., the span. In fact, like the Cloude–Pottier α – β model, our scattering vector model of (13) relies on the SU2-O3+ homomorphism that Cloude has used as basis of his ICTD [7], [31]. The special unitary constraint (i.e., $\det(U) = 1$) related to the SU2-O3 homomorphism [32] allowed Cloude to preserve the length of the original \vec{S}_d vector and to solve for the coneigenvalue phase ambiguity problem raised by several authors [23], [24], [33]. Our scattering vector model solves also for Huynen's skip angle ambiguity [24], and (13) should be used instead of (11) to derive unique and unambiguous scattering parameters α_s and Φ_{α_s} that are not affected by coneigenvalue phase ambiguity.

E. Representation of the Roll-Invariant Scattering Vector

As shown in Section II-B, elimination of the orientation angle ψ leads to a roll-invariant scattering vector $\vec{V}^{\text{orient-inv}}$,

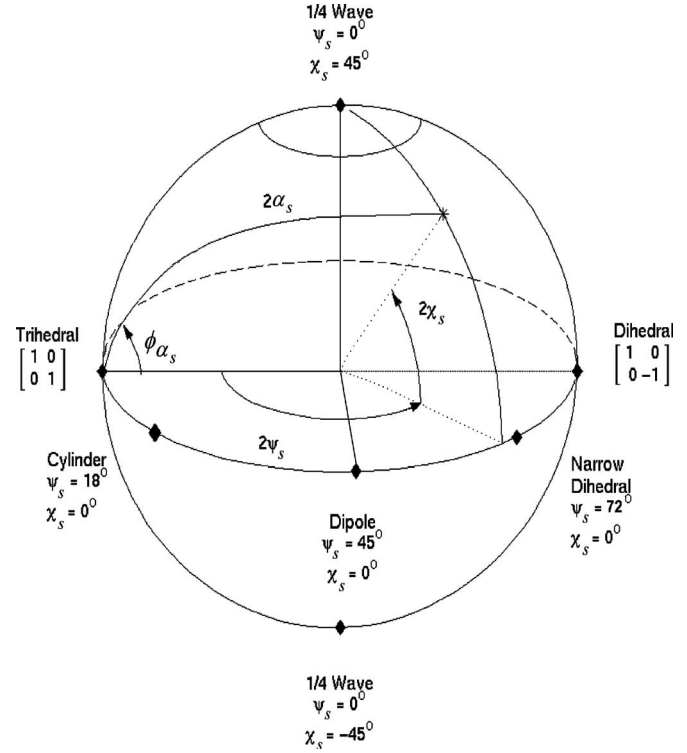


Fig. 1. Symmetric scattering target Poincaré sphere.

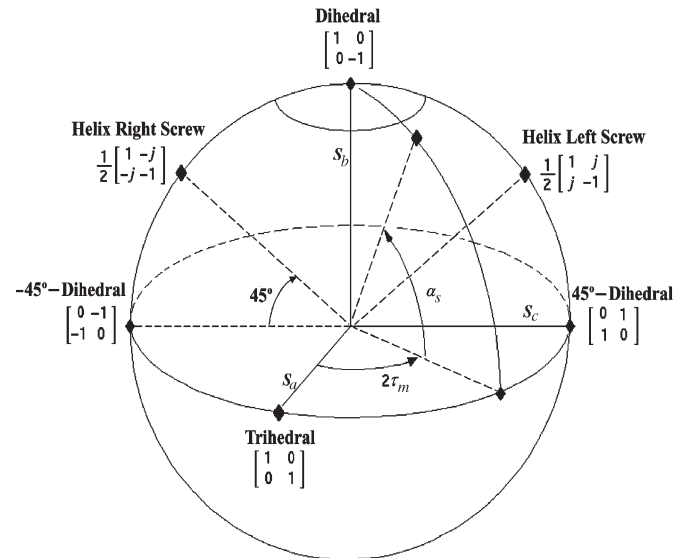


Fig. 2. Scattering type and helicity Poincaré sphere ($\alpha_s, \tau_m, \Phi_{\alpha_s} = 0$).

which can be expressed using (13) as a function of m , τ_m , α_s , and Φ_{α_s} , i.e.,

$$\vec{V}^{\text{orient-inv}} = m \cdot \begin{bmatrix} \cos \alpha_s \cos 2\tau_m, \sin \alpha_s e^{j\Phi_{\alpha_s}}, \\ -j \cos \alpha_s \sin 2\tau_m \end{bmatrix}^T. \quad (15)$$

To demonstrate the importance of α_s , Φ_{α_s} , and τ_m for an unambiguous description of coherent target scattering type, one parameter among the three is fixed, and this permits the use of the Poincaré sphere representations of Figs. 1 and 2 for mapping the normalized $\vec{V}^{\text{orient-inv}}$.

Fig. 1 presents the symmetric target Poincaré sphere [29], [34] for the representation of symmetric scatterers ($\tau_m = 0$). Each symmetric scatterer of scattering type parameters α_s and Φ_{α_s} is uniquely mapped as a point of latitude $2\psi_s$ and longitude $2\chi_s$ on the surface of the target Poincaré sphere of Fig. 1. ψ_s and χ_s can be derived from the $\vec{V}^{\text{orient-inv}}$ parameters $(\alpha_s, \Phi_{\alpha_s})$, as described in [29]. Notice the key role of the scattering type phase Φ_{α_s} for an unambiguous characterization of symmetric scatterers that are lying on the North and South hemispheres of the Poincaré sphere of Fig. 1. If Φ_{α_s} is ignored, only the points on the equator can be characterized with α_s , and symmetric scatterers of nonzero Φ_{α_s} cannot be separated from the equator scatterers of the same α_s .

The importance of the helicity for an unambiguous description of target scattering type can also be demonstrated using the unit Poincaré sphere of Fig. 2. The sphere covers only the target scatterers of in-phase $S_a S_b$ components of the trihedral–dihedral basis (S_a, S_b) , i.e., scatterers of zero symmetric scattering type phase $\Phi_{\alpha_s} = \Phi_{S_a} - \Phi_{S_b} = 0$. The unit length vector $(\cos \alpha_s \cos 2\tau_m, \sin \alpha_s, \cos \alpha_s \sin 2\tau_m)$, whose S_c component (third coordinate) is taken as the opposite of the imaginary part of the original $\vec{V}^{\text{orient-inv}}$ component in (15), may be used for a simplified representation of in-phase- $S_a S_b$ scatterers. Each scatterer can be mapped as a point of latitude $2\tau_m$ and longitude α_s on the unit Poincaré sphere of Fig. 2. Nonsymmetric targets (with $\Phi_{\alpha_s} = 0$) are now represented as separate and unique points on the Poincaré sphere. For example, the right and left helices, which have the same symmetric scattering type $\alpha_s = \pi/4$, are mapped on two different sphere locations due to the helicity information, i.e., $\tau_m = -\pi/4$ and $\tau_m = \pi/4$ for the right and left helices, respectively.

In summary, the three parameters τ_m , α_s , and Φ_{α_s} should be used for an unambiguous description of coherent target scattering type. In the following, the scattering vector model is used to assess the sensitivity of the Cloude–Pottier α – β model to the rotation ψ of the incidence plane about the LOS.

III. COMPARISON OF THE CLOUDE–POTTIER α – β MODEL WITH OUR SCATTERING VECTOR MODEL

A. Symmetric Target

Comparison of our scattering vector model of (13) with the Cloude–Pottier α – β model of (1) leads to the following observations for a symmetric scatterer ($\tau_m = 0$).

- The Cloude α angle is identical to α_s .
- β ($= 2\psi$), like ψ , provides pure measurement of the physical target tilt angle about the LOS.
- The scattering type phase Φ_{α_s} is identical to the phase difference $\phi_2 - \phi_1$.

Hence, our scattering vector model and the Cloude–Pottier α – β model provide the same information for a symmetric scatterer.

Notice that the phase difference $\phi_2 - \phi_1$, which is denoted as δ in [3], has been derived in [2] and [3] for azimuthally symmetric natural targets. For such targets, δ was interpreted as a measure of the relative magnitude of HH and VV, which may be used to separate the Bragg surface from multiple scattering mechanisms [2], [3], [15]. However, δ has never been used since for scattering type description and as mentioned

by Pottier *et al.* [15], “the main parameter used for scattering type identification is α because of its roll-invariant property [15].” In Section V, Convair-580 SAR data will be used to demonstrate that both the magnitude α_s and phase Φ_{α_s} of the symmetric scattering type should be used for an unambiguous description of symmetric and asymmetric target scattering. The additional information provided by Φ_{α_s} (or δ) should improve significantly the Cloude–Pottier bidimensional H/α scattering classification [9] for symmetric targets. For asymmetric scattering, δ , which is not roll invariant as shown in the Section III-B, cannot be used for scattering type description, and the scattering vector model parameters α_s , Φ_{α_s} , and τ_m are required for an unambiguous description of target scattering type.

B. Nonsymmetric Target

For nonsymmetric targets (i.e., $\tau_m \neq 0$), the Cloude–Pottier α – β model and our scattering vector model lead to different parameters, and the comparative study of the two models leads to the following conclusions.

- β no longer provides pure measurement of the physical target orientation. In fact, β is a function of the target orientation angle ψ , the target helicity τ_m , and the symmetric scattering type vector parameters α_s and Φ_{α_s} . Fig. 3 presents α and $\beta/2$ variations as a function of α_s for a zero orientation asymmetric target ($\psi = 0$, $\tau_m = \pi/8$, and $\Phi_{\alpha_s} = 0$). The β measure is biased toward higher values with a bias that increases with increasing τ_m , as shown in Fig. 4. The latter one presents α and $\beta/2$ variations as a function of τ_m for a zero orientation target ($\psi = 0$, $\alpha_s = \pi/4$, and $\Phi_{\alpha_s} = 0$). The bias on β of Figs. 3 and 4 might explain the erroneous azimuth slope measurements obtained from β in [16].
- α and α_s provide different information. In fact, the scattering type α is a function of α_s and the helicity τ_m , as shown in Figs. 3 and 4. Since both α_s and τ_m are roll invariant, α is roll invariant. However, scattering ambiguities might occur if only α is used for scattering type classification, as noted in [18] and discussed in Section II-E. For example, the helix and dihedral, which have the same scattering type $\alpha = 90^\circ$, cannot be separated. In this case, β and $\phi_2 - \phi_3$ should be used to remove the ambiguity [35], [36]. Therefore, β , which is needed for target tilt-angle measurement, is also required for characterization of asymmetric scattering type. This might lead to erroneous scattering classification in the presence of tilted targets, and erroneous tilt-angle measurements if the scattering type contribution were not retrieved from β .
- Even though α and Φ_1 are invariant with the antenna basis rotation ψ about the LOS, β , Φ_2 , and Φ_3 do vary with ψ . Therefore, the α – β model parameterization is not polarization wave basis invariant, and this explains the different parameter values obtained by Corr and Rodrigues [18] when they used the sphere–helix basis as an alternative to the Pauli basis. The “new” β and phase parameters Φ_i derived in the sphere–helix basis allowed Corr and Rodrigues to resolve certain scattering type ambiguities that occur with the Pauli-basis Cloude–Pottier parameters [18].

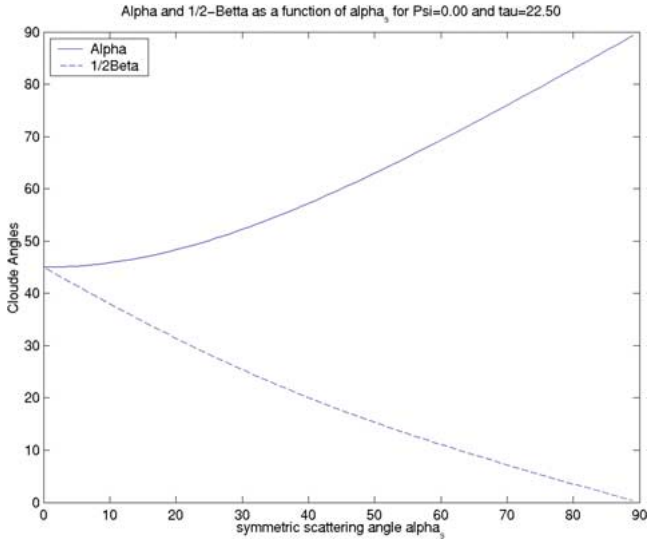


Fig. 3. α and $\beta/2$ variations as functions of α_s for a zero-oriented symmetric scatterer and $\Phi_{\alpha_s} = 0$.

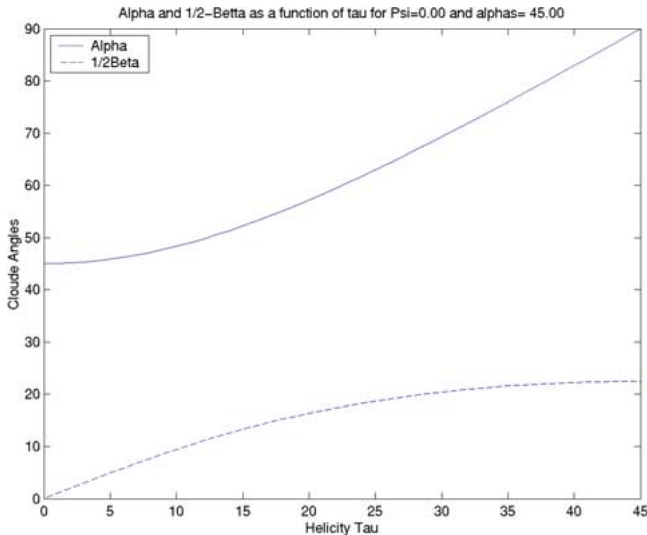


Fig. 4. α and $\beta/2$ variations as functions of τ_m for a zero-oriented symmetric scatterer and $\alpha_s = 45^\circ$, $\Phi_{\alpha_s} = 0$.

In summary, our scattering vector model and the Cloude–Pottier α – β model provide identical parameters for a symmetric scatterer. Consequently, all the interesting results widely published on symmetric targets with the Cloude ICTD H/α classification can be extended to the scattering vector model. The use of Φ_{α_s} as a third dimension in addition to the Cloude–Pottier bidimensional scattering plane should provide significant improvement for symmetric target scattering classification, as illustrated in Section V-B. For nonsymmetric targets, certain parameters provided by the α – β model do depend on the target orientation, whereas the scattering vector model parameters are still polarization basis invariant (i.e., roll invariant). In order to take full advantage of both Kennaugh–Huynen’s basis-invariant target theory [5], [6] and Cloude’s ICTD theory [1], [7], the scattering vector model is integrated into Cloude’s ICTD to derive a new ICTD. Our scattering vector model of (13) also served as basis for the development of a roll-invariant CTD, as discussed in Section IV.



Fig. 5. Convair-580 multipolarization SAR image (Ottawa, ON, Canada). (Red) HH. (Green) HV. (Blue) VV.

IV. UNIQUE AND ROLL-INVARIANT COHERENT AND INCOHERENT TARGET SCATTERING DECOMPOSITION

A. Unique and Roll-Invariant CTD

The scattering vector model is used as the basis of unique and roll-invariant coherent target scattering decomposition. The new CTD is applied to each single-look pixel scattering $[S]$ matrix. $[S]$ is con-diagonalized and represented in terms of the scattering vector model parameters ψ , τ_m , m , α_s , and Φ_{α_s} , as discussed in Section II-D. These parameters, which do not depend on the wave polarization basis, are target characteristics and permit a unique and roll-invariant decomposition of coherent target scattering. The roll-invariant CTD provides an unambiguous description of the symmetric target scattering type using the complex scattering type parameters α_s and Φ_{α_s} . The helicity τ_m permits the measurement of the degree of target scattering symmetry. The combination of τ_m with m and ψ leads to a full characterization of the maximum target return.

It is worth noting that the Krogager CTD [8], [37] is also roll invariant. This method decomposes target scattering into three coherent components that have physical interpretation in terms of dihedral, sphere, and helical targets [37]. However, even though the Krogager CTD leads to interesting classifications, the decomposition is not completed in an orthogonal basis, and as a result, the elements of the decomposition are not basis invariant [3]. In contrast to the Krogager CTD, our CTD is conducted in the orthonormal Pauli basis, and this leads to a unique and roll-invariant decomposition of coherent target scattering.

Notice that the parameters of the unique and roll-invariant CTD have already been validated for targets of significant symmetric scattering, using the SSCM [29]. α_s and Φ_{α_s} have been shown to be very promising for ship recognition [30], [38]. The maximized target symmetric scattering parameters α_s and Φ_{α_s} permit the identification of permanent symmetric scatterers on the ship under study, with stable complex symmetric scattering parameters under different wind and sea conditions [30], [38]. This leads to the extraction of a ship-specific distribution—ship signature—of permanent quasi-symmetric scatterers (i.e., scatterer of significant symmetric scattering component). Their orientation angle ψ permit an accurate ship pitch angle

measurement provided that the SAR system is corrected for focus setting and Doppler centroid errors [30].

All the SSCM promising results [29], [30], [38] were obtained using quasi-symmetric point target of sufficiently high signal-to-clutter ratio or extended targets that pass the SSCM target coherence test [29]. The maximum intensity m was used as the basis for the point target coherence test introduced in [29]. For more general applications that involve both symmetric and asymmetric targets, our CTD is more suitable than the SSCM. However, like the SSCM, the new CTD should be limited to the decomposition of coherent target scattering, which is fully characterized with single-look scattering matrix measurement. Targets, which exhibit significant natural variability in their scattering properties, are generally characterized with the Mueller matrix, covariance or coherency matrix that preserves the full polarimetric information provided by the time-varying parameters [2]–[4], [39], [40]. ICTD is required for the decomposition of these targets, which were named partially coherent targets in [40]. In the following, the scattering vector model is used as the basis for the development of a unique and roll-invariant ICTD.

B. Roll-Invariant ICTD

The roll-invariant ICTD has been inspired from the Cloude–Pottier ICTD [3], [7]. For a reciprocal target, the characteristic decomposition of the Hermitian positive semidefinite target coherency matrix $[T]$ permits a unique representation of $[T]_i$ as the incoherent sum of up to three coherency matrices $[T]_i$ representing three different single scatterers, each weighted by its appropriate positive real (noncomplex) eigenvalue λ_i [7], i.e.,

$$[T] = \sum_{i=1,3} \lambda_i [T]_i. \quad (16)$$

Each single scattering i ($i = 1, 3$) is represented by the coherency eigenvector matrices $[T]_i$ of rank 1 and the corresponding normalized positive real eigenvalue $\lambda_i/(\lambda_1 + \lambda_2 + \lambda_3)$, which is a measure of the relative energy carried by the eigenvector i .

The roll-invariant ICTD will be applied as follows.

- 1) Compute the target coherency matrix $[T]$ within a moving window.
- 2) Diagonalize the target coherency matrix and provide the three eigenvectors and the corresponding eigenvalues.
- 3) Apply the scattering vector model of (13) for a unique and roll-invariant parameterization of the three eigenvectors. Each eigenvector i , which corresponds to a single scattering, is presented in terms of the scattering vector model basis-invariant parameters as follows:

$$\text{ICTD}_i = (\lambda_i, m_i, \psi_i, \tau_{mi}, \alpha_{si}, \Phi_{\alpha_{si}}). \quad (17)$$

Target scattering can be fully characterized by a deep analysis of each of the three eigenvector parameters of (17). For a global analysis of the target “average” scattering [3], [9], averaged (weighted by the eigenvalues) parameters can be derived from the separate eigenvector parameters, as done in [3] and [9], at

the risk of loss of useful target scattering information. The normalized eigenvalues, which are identical to the ones generated by Cloude–Pottier’s ICTD, may also be combined to derive the entropy and anisotropy [3], [9] for the characterization of target scattering heterogeneity.

However, like the Cloude–Pottier ICTD, our ICTD may be affected by speckle [19], [40]–[42]. The presence of speckle may introduce biases on the ICTD parameters derived from the characteristic decomposition of the coherency matrix sample. The coherency eigenvalues and entropy estimates can be significantly biased [41], [42]. Recently, we have shown [42] using Convair-580 SAR data that the coherency eigenvector parameters and, in particular, the scattering type α_s and α may also be significantly biased with a bias that decreases with increasing processing window size. We have shown in [42] that the statistics of cross-channel coherence derived for circular complex Gaussian processes [43] can be used to determine the minimum processing window size required for an unbiased estimation of the ICTD decomposition parameters. A processing window that includes a minimum of 60 independent samples is required for an unbiased ICTD [41], [42]. Therefore, ICTD should be limited to coarse resolution applications, whereas high-resolution CTD should be limited to coherent targets of sufficiently high signal-to-noise ratio, as discussed previously.

V. ILLUSTRATION USING CONVAIR-580 SAR DATA: RESULTS AND DISCUSSIONS

A. Comparison of Our Roll-Invariant ICTD and the Cloude–Pottier ICTD

Several polarimetric Convair-580 C-band SAR [20] data sets collected over Ottawa, ON, Canada, and Mer Blue (in the east of Ottawa) are used for validation of the preceding results. For an unbiased estimation of the ICTD, a processing window of about 60 independent looks [41], [42] is used to calculate the spatially varying multilook target coherency matrix. The latter one is then diagonalized to derive the roll-invariant ICTD parameters and the Cloude ICTD parameters associated to each image pixel. In this section, the Ottawa scene of Fig. 5, which includes urban areas, farm fields, and forested areas, is used. First, the dominant and the second eigenvector scattering parameters are analyzed. The roll-invariant ICTD parameters of the global or average (weighted by the eigenvalues) scattering are considered in the last part of this section. Only the scattering type magnitude and the helicity are considered in this part, and the space-averaged parameters of the global scattering are denoted as α_{sg} and τ_{mg} (the index g for the global or average scattering).

The dominant scattering roll-invariant target parameters α_{s1} , $\phi_{\alpha_{s1}}$, and τ_1 are presented in Fig. 6. Most of the areas in the scene are of quasi-symmetric scattering with a helicity τ_1 of within $\pm\pi/12$, with the exception of a few isolated asymmetric scatterers in the urban and forested areas. τ_1 , which also represents the degree to which the Cloude scattering type α_1 deviates from α_{s1} , allows us to conclude that our ICTD and the Cloude–Pottier ICTD are generally similar for the Ottawa scene, which is dominated by targets of symmetric scattering: $\tau_1 \simeq 0$ and $\alpha_1 \simeq \alpha_{s1}$. Comparison of the dominant scattering

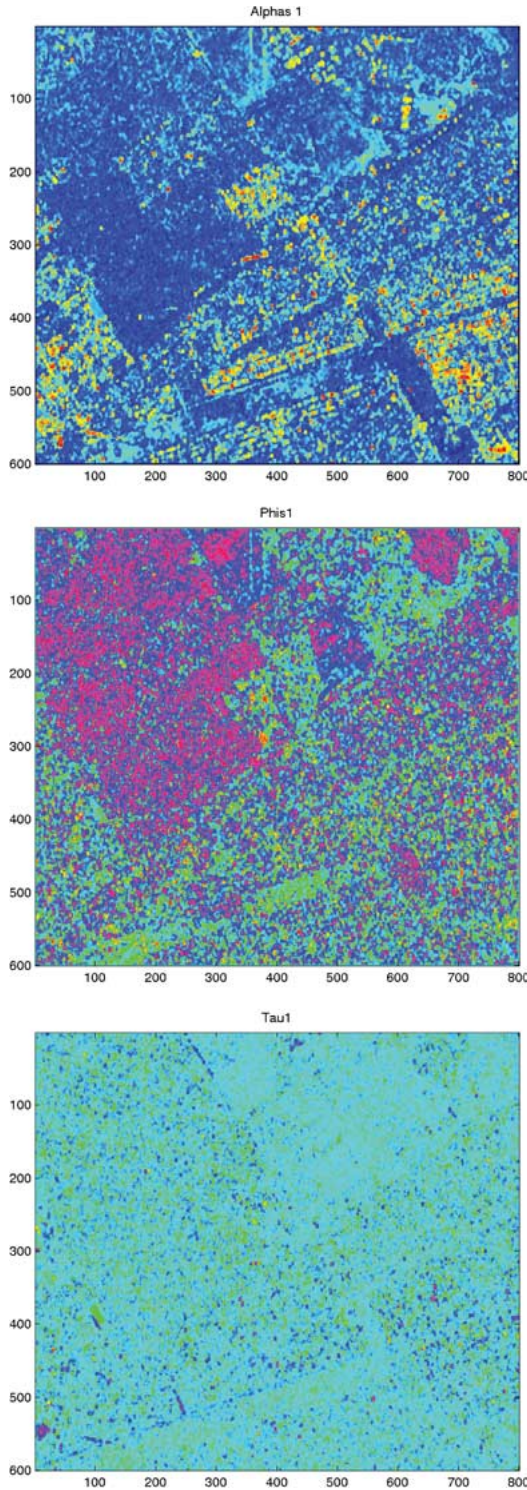


Fig. 6. Dominant scattering type and helicity. (Top) α_{s1} . (Middle) $\phi_{\alpha_{s1}}$. (Bottom) τ_1 .

type magnitude α_{s1} (or α_1) with the HH–HV–VV image of Fig. 5 reveals some weakness related to the scattering type description; whereas α_{s1} (and α_1) cannot discriminate the farm fields from forested areas, the multipolarization image does, as shown in Fig. 5. Such weakness is recovered when the phase information provided by the symmetric scattering type phase $\phi_{\alpha_{s1}}$ is used as seen in Fig. 6. The key role of the scattering type phase information for a complete characterization of target

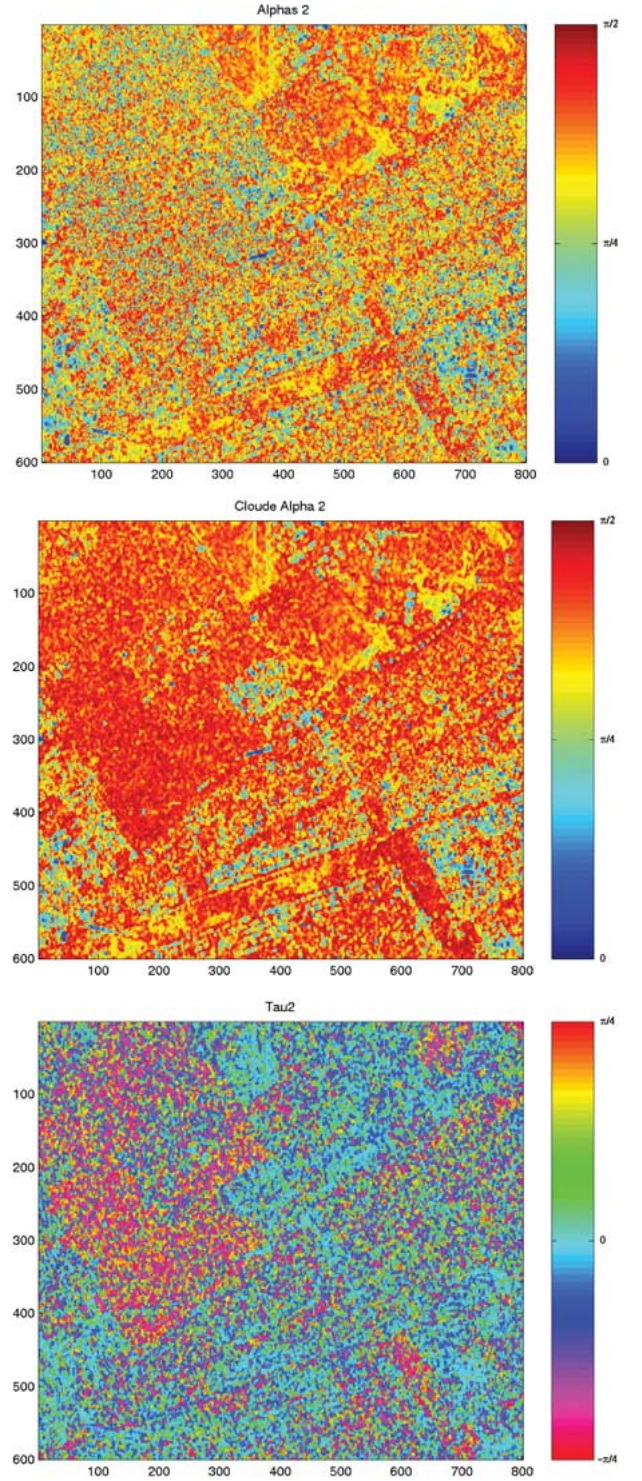


Fig. 7. Second scattering type magnitude and helicity. (Top) α_{s2} . (Middle) Cloude α_2 . (Bottom) τ_2 .

scattering type will be confirmed for wetland classification in Section V-B.

As discussed in Section III-B, the scattering vector model and the Cloude–Pottier α – β model should lead to different results in the presence of asymmetric scattering and, as a result, to different ICTDs. The second eigenvector scattering (corresponding to λ_2 , with $\lambda_3 < \lambda_2 < \lambda_1$), which has demonstrated the presence of significant asymmetric scattering, should be

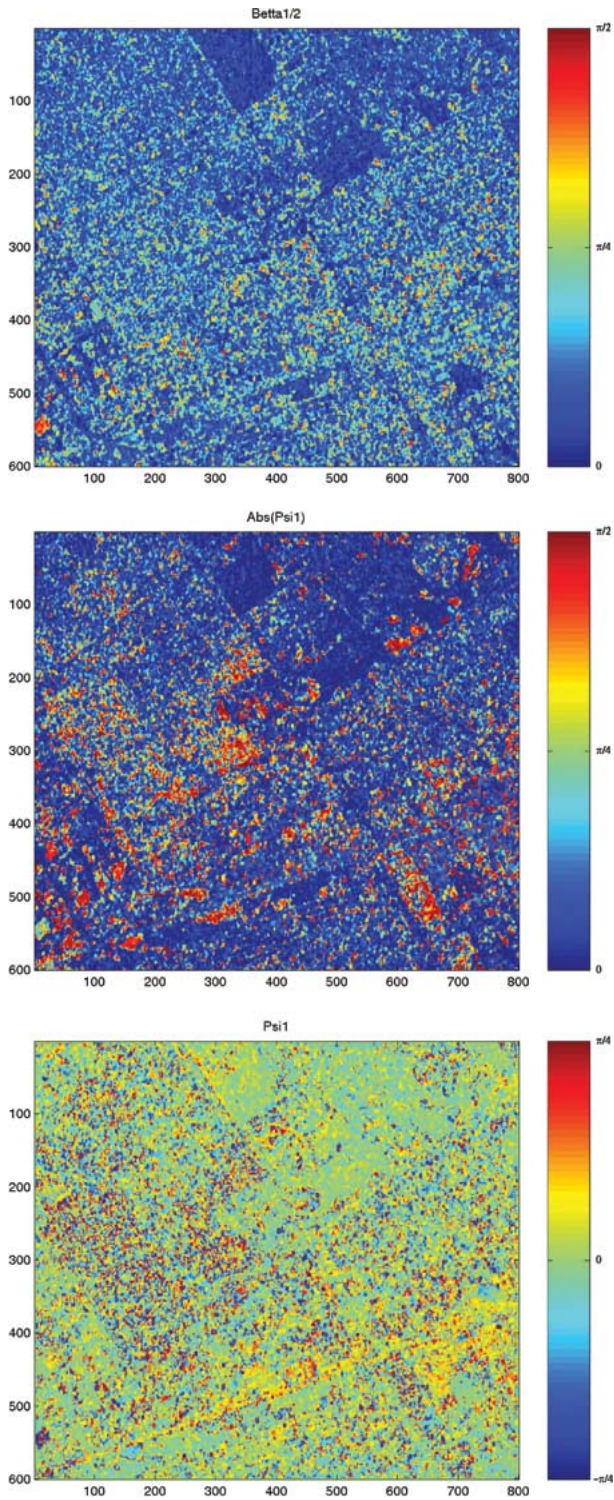


Fig. 8. Measurement of orientation angle. (Top) $\beta_1/2$. (Middle) $|\psi_1|$. (Bottom) With ψ_1 ambiguity removed.

suitable for a fair comparison between the roll-invariant ICTD and the Cloude–Pottier ICTD. Fig. 7 presents, for the second eigenvector scattering, the symmetric scattering type α_{s2} , the Cloude scattering type α_2 , and the helicity τ_2 . The second single scattering behaves generally as an asymmetric scattering, with the exception of farm fields, as shown in the τ_2 image of Fig. 7. The use of target helicity τ_2 permits separating symmetric from asymmetric scatterers that have the same scattering

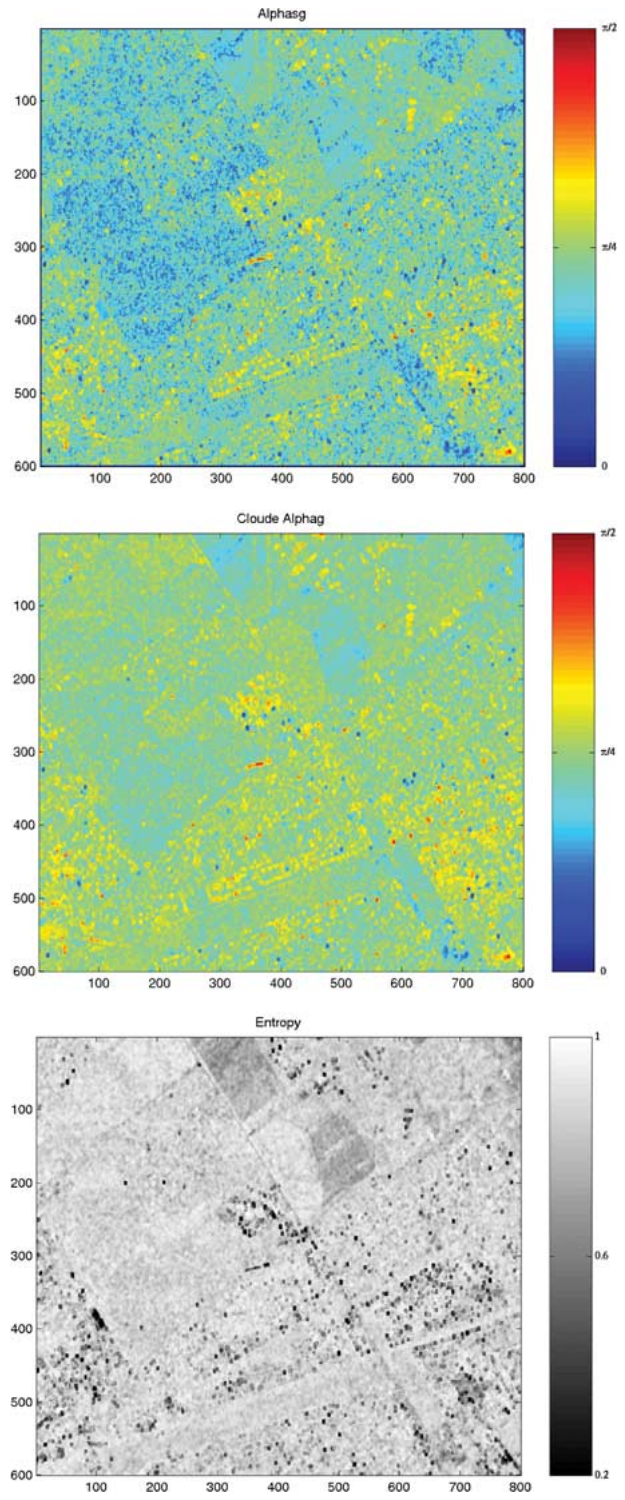


Fig. 9. Target global scattering parameters. (Top) α_{sg} . (Middle) Cloude α_g . (Bottom) H .

type α_2 . As a result, ambiguous symmetric and nonsymmetric scatterers of the same α_2 value, such as the helical and dihedral scattering of $\alpha_2 = 90^\circ$, are now well separated in the τ_2 and α_{s2} of Fig. 7. Notice that the moving cars (annotated in Fig. 5) on the top right of Fig. 7 of $\alpha_2 = 90^\circ$ are now assigned to symmetric ($\tau_2 = 0$) dihedral scattering. Notice also that the forest area on the top left of Fig. 7, which is annotated in Fig. 5, manifests a second scattering that is dominated by the helical

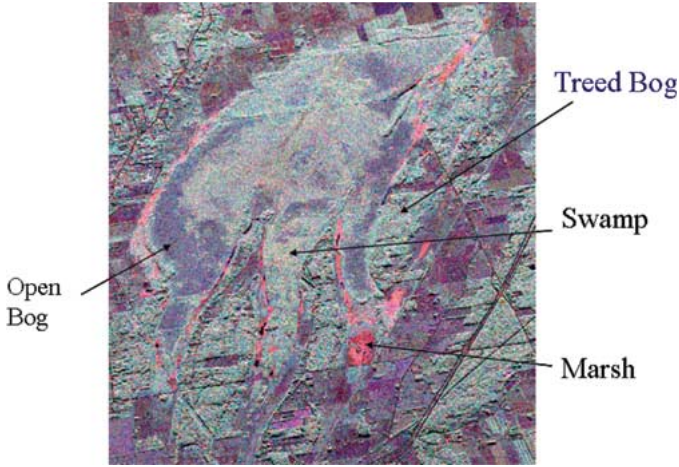


Fig. 10. Convair-580 multipolarization SAR image (Mer Bleue). (Red) HH. (Green) HV. (Blue) VV.

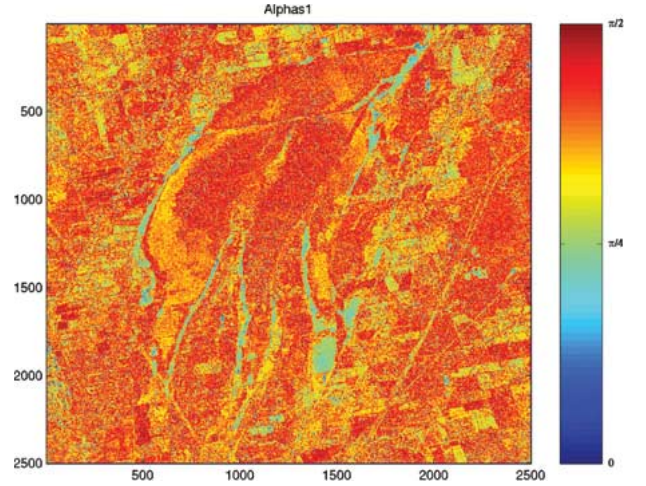


Fig. 12. Dominant scattering type magnitude.

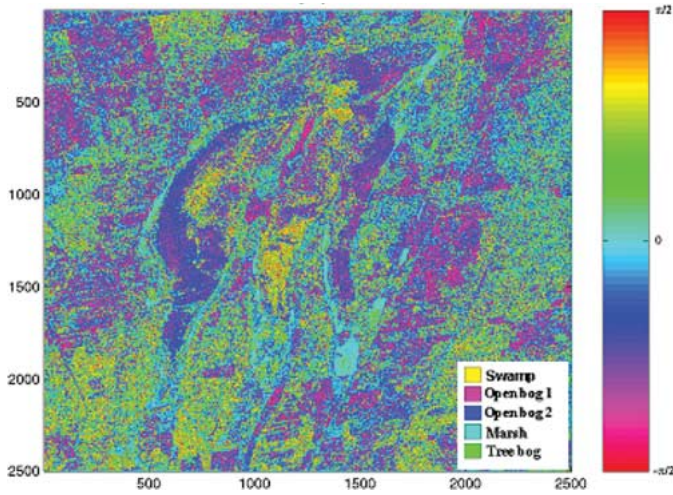


Fig. 11. Dominant scattering type phase.

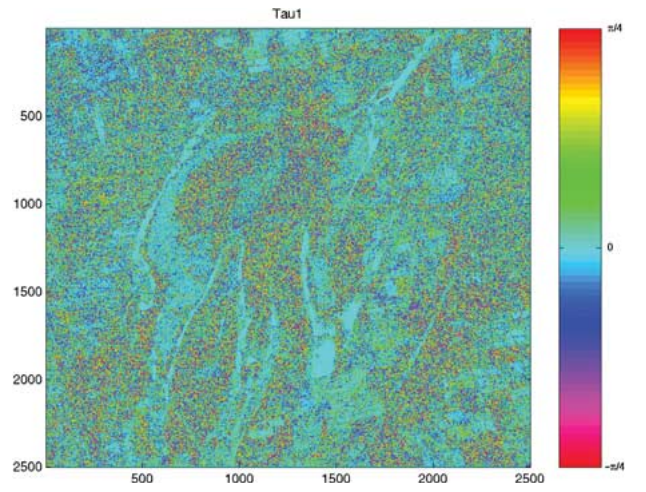


Fig. 13. Dominant scattering type helicity.

scattering $\tau_2 \simeq \pi/2$. This area of high helicity, which appears in the Cloude α_2 image as an area of “homogeneous” scattering ($\alpha_2 \simeq \pi/2$), demonstrates in fact a spatially “heterogeneous” scattering according to α_{s2} . The removal of the scattering type ambiguities related to α_2 description reveals the significant spatial scattering variations of the forest area, and this explains the large spatial variations of α_2 in comparison with the nearly uniform but ambiguous α_2 .

The orientation angle should also highlight the difference between our ICTD and the Cloude–Pottier ICTD. In Section III, it was shown that the Cloude orientation angle β is twice the orientation angle ψ for symmetric targets. The orientation angle of the dominant scattering is calculated for the Ottawa flat scene. $\beta_1/2$, $|\psi_1|$, and the orientation angle ψ_1 [after ambiguity removal (14)] are presented in Fig. 8. Even though the helicity τ_1 of Fig. 6 is close to zero (within $\pm\pi/12$), a large difference can be noted between $\beta_1/2$ and $|\psi_1|$. In comparison with $|\psi_1|$, $\beta_1/2$ is biased toward higher values, as discussed in Section III-B and confirmed in Fig. 8. $|\psi_1|$ manifests a dominant dark blue mainly in the flat and symmetric flat farm fields, and this indicates a target tilt angle close to zero. The same areas manifests a nonzero β_1 , and this corresponds to a bias in the

tilt-angle measure that was first raised in [16]. Notice that in the $|\psi_1|$ image, the $\pm\pi/2$ ambiguity in the orientation measure is now removed in the ψ_1 image using (14), with an orientation measure lying within the interval $[-\pi/4, \pi/4]$. In a future study, the ICTD orientation angle ψ will be further investigated for intrinsic tilt target angle measurements.

For a global analysis of the average scattering [9], the roll-invariant ICTD eigenvalue weighted parameters are derived for the Ottawa scene. The entropy H , which characterizes scattering heterogeneity [3], [9], our ICTD α_{sg} , and the Cloude–Pottier ICTD α_g are presented in Fig. 9. As might be expected, the average symmetric scattering type magnitude α_{sg} performs better than the dominant scattering α_{s1} of Fig. 6 in terms of farm field and forested areas discrimination. α_{sg} , which also demonstrates larger dynamic range than the Cloude α_g , looks to be more promising for target discrimination. In the future, the information provided by the average scattering parameters H , α_{sg} , and τ_{mg} will be combined and investigated for a deeper target scattering classification. The complementary information provided by the dominant scattering phase $\phi_{\alpha_{s1}}$ and orientation ψ_1 will also be considered for a better target scattering classification.

B. Roll-Invariant ICTD Scattering Type Phase Information for Wetland Classification

Our roll-invariant ICTD has also been investigated for wetland classification. Convair-580 polarimetric C-band SAR and *in situ* data were collected over the Mer Bleue wetland site in June 1995. Fig. 10 presents the multipolarization HH–HV–VV image (HH in red, HV in green, and VV in blue). Four Mer Blue wetland classes are identified using aerial photos and ground truth data: open and treed bog, marshes, and swamp. The roll-invariant ICTD is applied on the Mer Blue image with a moving window of approximately 60 independent looks. The dominant scattering parameters $\phi_{\alpha_{s1}}$, α_{s1} , and τ_1 are presented in Figs. 11–13. As shown in Fig. 11, $\phi_{\alpha_{s1}}$ permits an immediate and quite efficient unsupervised classification of the Mer Bleue wetland into the four wetland classes previously discussed. $\phi_{\alpha_{s1}}$ also permits a clear discrimination within the open bog class between small shrubs (in magenta) and sedges (in dark blue), leading to the subclasses open bog 1 and 2. In contrast to the symmetric scattering type phase, the symmetric scattering type magnitude α_{s1} of Fig. 12 has poor potential in wetland class discrimination and performs worse than the multipolarization HH–HV–VV of Fig. 10. This is due to the fact that the C-band scattering type α_{s1} , which is identical to the Cloude α for symmetric scattering $\tau \simeq 0$ in Fig. 13, is not effective for vegetation-type discrimination. Such a result is in agreement with one of our previous studies [44], in which we demonstrated that the Cloude α is not effective for forest-type discrimination. Other polarimetric tools, such as the circular polarizations and the degree of polarization extrema, were more successful and permit the enhancement of forest-type discrimination even under leafy conditions [44]. The use of the phase information of the complex symmetric scattering type $\phi_{\alpha_{s1}}$ provides the key information missed by α_{s1} for an enhanced vegetation-type discrimination and wetland classification, as shown in Fig. 11. Notice that in the helicity image of Fig. 13, the marsh and open bog classes are dominated by symmetric scattering, while the tree bog and swamp classes manifest a significant asymmetric scattering component. In the future, the helicity will be combined with the complex scattering type magnitude and phase and the orientation ψ for an improved wetland classification. All the parameters of our roll-invariant ICTD will be further studied and validated for wetland indicator measurement, in preparation for the operational use of RADARSAT-2 for Canadian wetland monitoring.

VI. CONCLUSION

The scattering vector model introduced in this paper permits a unified decomposition of coherent and partially coherent target scattering. This model is used as the basis for the development of a unique and roll-invariant CTD, which can be applied for the characterization of coherent target scattering. Partially coherent targets, which exhibit significant natural variability in their scattering properties, can be characterized using our new ICTD. The roll-invariant ICTD, which is inspired from the Cloude–Pottier ICTD, uses the scattering vector model for the eigenvector parametrization, and this leads to a unique and roll-invariant decomposition of partially coherent target scattering

in terms of target characteristics. For symmetric scattering, our ICTD and the Cloude–Pottier ICTD lead to identical scattering decomposition. Consequently, all the interesting results widely published on symmetric targets with the Cloude ICTD H/α classification can be extended to our ICTD. The use of the scattering type phase information Φ_{α_s} , in addition to that provided by the scattering type magnitude α_s , is essential for an unambiguous description of target scattering. For asymmetric targets, certain parameters provided by the Cloude–Pottier ICTD do depend on the polarization basis, whereas our ICTD parameters remain roll invariant. The Cloude α scattering type description may be ambiguous at the presence of asymmetric scattering, as noted in [18]. Such ambiguities are solved with our ICTD, which uses the helicity in addition to the symmetric scattering type parameters α_s and Φ_{α_s} for a complete and unique representation of target scattering.

Like the Cloude–Pottier ICTD, our ICTD should be limited to coarse resolution applications. The presence of speckle leads to biased ICTD parameters, and a processing window that contains a minimum of 60 independent looks is required for an unbiased ICTD [45]. We have previously recommended [29], [40] the use of a mixture of high-resolution CTD and coarse-resolution ICTD for optimum analysis of coherent and partially coherent target scattering that might occur in the same SAR scene. Our scattering vector model permits a unified and roll-invariant decomposition of both coherent and partially coherent target scattering in terms of unique target characteristics. A mixed coherent–incoherent target decomposition based on our scattering vector model is currently being developed. This should lead to a unique and roll target scattering decomposition, which preserves the high-resolution coherent target scattering information as well as the full polarimetric information provided by the coherency characteristic decomposition of partially coherent target scattering.

ACKNOWLEDGMENT

The author would like to thank the anonymous reviewers for the helpful comments and suggestions. R. Gauthier (CCRS) is thanked for having organized the Mer Bleue Convair-580 campaign in 1995 and having provided us with the required ground truth data and helpful comments. The Canadian Space Agency is thanked for having partially funded the present study.

REFERENCES

- [1] S. R. Cloude, “Uniqueness of target decomposition theorems in radar polarimetry,” in *Proc. NATO Adv. Res. Workshop Direct and Inverse Methods Radar Polarimetry*, W.-M. Boerner *et al.*, Ed. Dordrecht, The Netherlands: Kluwer, 1992, vol. 350, pp. 267–296. Sep. 1988; p. 1938.
- [2] J. J. Van Zyl, “Application of Cloude’s target decomposition theorem to polarimetric imaging radar data,” in *Proc. SPIE*, H. Mott and W.-M. Boerner, Eds, San Diego, CA, Jul. 1992, vol. 1748, pp. 184–191.
- [3] S. R. Cloude and E. Pottier, “A review of target decomposition theorems in radar polarimetry,” *IEEE Trans. Geosci. Remote Sens.*, vol. 34, no. 2, pp. 498–518, Mar. 1996.
- [4] W. M. Boerner, H. Mott, E. Luneburg, C. Livingstone, B. Brisco, R. J. Brown, and J. S. Paterson, “Polarimetry in radar remote sensing: Basic and applied concepts,” in *Manual of Remote Sensing: Principles and Applications of Imaging Radar*, vol. 3, R. A. Ryerson, Ed. Hoboken, NJ: Wiley, 1998, ch. 5, pp. 271–356. with contributions by S. R. Cloude,

- E. Krogager, J. S. Lee, D. L. Schuler, J. J. van Zyl, D. Randall, P. Budkewitsch, and E. Pottier.
- [5] K. Kennaugh, "Effects of type of polarization on echo characteristics," Ohio State Univ., Antenna Lab., Columbus, OH, Tech. Rep. 389-4, 381-9, 1951.
- [6] J. R. Huynen, "Measurement of the target scattering matrix," *Proc. IEEE*, vol. 53, no. 8, pp. 936-946, Aug. 1965.
- [7] S. R. Cloude, "Group theory and polarization algebra," *Optik*, vol. 75, no. 1, pp. 26-36, 1986.
- [8] E. Krogager and Z. H. Czyz, "Properties of the sphere, diplane, helix decomposition," in *Proc. 3rd Int. Workshop Radar Polarimetry (JIPR)*, Mar. 21-23, 1995, pp. 106-114.
- [9] S. R. Cloude and E. Pottier, "An entropy based classification scheme for land applications of polarimetric SARs," *IEEE Trans. Geosci. Remote Sens.*, vol. 35, no. 1, pp. 68-78, Jan. 1997.
- [10] J. S. Lee, M. R. Grunes, T. L. Ainsworth, L. Du, D. L. Schuler, and S. R. Cloude, "Unsupervised classification of polarimetric SAR images by applying target decomposition and complex Wishart distribution," *IEEE Trans. Geosci. Remote Sens.*, vol. 37, no. 5, pp. 2249-2258, Sep. 1999.
- [11] E. Pottier and J. S. Lee, "Application of the H/A/ α polarimetric decomposition theorem for unsupervised classification of fully polarimetric SAR data based on the Wishart distribution," in *Proc. CEOS Workshop*, Toulouse, France, 1999, pp. 335-340.
- [12] L. Ferro-Famil, E. Pottier, and J. S. Lee, "Unsupervised classification of multifrequency and fully polarimetric SAR images based on the H/A/Alpha-Wishart classifier," *IEEE Trans. Geosci. Remote Sens.*, vol. 39, no. 11, pp. 2332-2342, Nov. 2001.
- [13] I. Hajsek, E. Pottier, and S. R. Cloude, "Inversion of surface parameters from polarimetric SAR," *IEEE Trans. Geosci. Remote Sens.*, vol. 41, no. 4, pp. 727-744, Apr. 2003.
- [14] S. R. Cloude, "Wide band polarimetric radar inversion studies using the entropy-alpha decomposition," *Proc. SPIE*, vol. 3120, pp. 118-129, 1997.
- [15] E. Pottier, D. L. Schuler, J.-S. Lee, and T. A. Ainsworth, "Estimation of the terrain surface azimuthal-range slopes using polarimetric decomposition of POLSAR data," in *Proc. IGARSS*, Hamburg, Germany, 1999, pp. 2212-2214.
- [16] J. S. Lee, D. L. Schuler, and T. L. Ainsworth, "Polarimetric SAR data compensation for terrain azimuth slope variation," *IEEE Trans. Geosci. Remote Sens.*, vol. 38, no. 5, pp. 2153-2163, Sep. 2000.
- [17] J. S. Lee, D. L. Schuler, D. L. Ainsworth, E. Krogager, D. Kasilingam, and W. M. Boerner, "On the estimation of radar polarization orientation shifts induced by terrain slopes," *IEEE Trans. Geosci. Remote Sens.*, vol. 40, no. 1, pp. 30-41, Jan. 2002.
- [18] D. G. Corr and A. F. Rodrigues, "Alternative basis matrices for polarimetric decomposition," in *Proc. EUSAR 2002*, Cologne, Germany, 2002, pp. 597-600.
- [19] R. Touzi, "Target scattering decomposition of one-look and multi-look SAR data using a new coherent scattering model: The TSVM," in *Proc. IGARSS*, Anchorage, AK, 2004, pp. 2491-2494.
- [20] C. E. Livingstone, A. L. Gray, R. K. Hawkins, P. W. Vachon, T. I. Lukowski, and M. LaLonde, "The CCRS airborne SAR systems: Radar for remote sensing research," *Can. J. Remote Sens.*, vol. 21, no. 4, pp. 468-491, 1995.
- [21] T. Takagi, "On an algebraic problem related to an analytical theorem of Caratheodory and Fejer and on an allied theorem of Landau," *Jpn. J. Math.*, vol. 1, pp. 83-93, 1927.
- [22] W. M. Boerner, M. B. El-Arini, C.-Y. Chan, and P. M. Mastoris, "Polarization dependence in electromagnetic inverse problems," *IEEE Trans. Antennas Propag.*, vol. AP-29, no. 2, pp. 262-271, Mar. 1981.
- [23] A. B. Kostinski and W. M. Boerner, "On foundation of radar polarimetry," *IEEE Trans. Antennas Propag.*, vol. AP-34, no. 12, pp. 1395-1404, Dec. 1986.
- [24] E. Luneburg, "Aspects of radar polarimetry," *Elektrik-Turkish J. Electr. Eng. Comput. Sci.*, vol. 10, no. 2, pp. 219-243, 2002.
- [25] J. R. Huynen, "Phenomenological theory of radar targets," Univ. Technol., Delft, Delft, The Netherlands, 1970. Tech. Rep. 43212.
- [26] R. Schmeider, "Stokes algebra formalism," *J. Opt. Soc. Amer.*, vol. 59, no. 3, pp. 297-302, 1969.
- [27] R. Touzi, C. E. Livingstone, J. R. C. Lafontaine, and T. I. Lukowski, "Consideration of antenna gain and phase patterns for calibration of polarimetric SAR data," *IEEE Trans. Geosci. Remote Sens.*, vol. 31, no. 6, pp. 1132-1145, Nov. 1993.
- [28] W. L. Cameron, N. Youssef, and L. K. Leung, "Simulated polarimetric signatures of primitive geometrical shapes," *IEEE Trans. Geosci. Remote Sens.*, vol. 34, no. 3, pp. 793-803, May 1996.
- [29] R. Touzi and F. Charbonneau, "Characterization of target symmetric scattering using polarimetric SARs," *IEEE Trans. Geosci. Remote Sens.*, vol. 40, no. 11, pp. 2507-2516, Nov. 2002.
- [30] R. Touzi, R. K. Raney, and F. Charbonneau, "On the use of symmetric scatterers for ship characterization," *IEEE Trans. Geosci. Remote Sens.*, vol. 42, no. 2, pp. 2039-2045, Oct. 2004.
- [31] S. R. Cloude, "Lie groups in electromagnetic wave propagation and scattering," *J. Electromagn. Waves Appl.*, vol. 6, no. 8, pp. 947-974, 1992.
- [32] G. B. Arfken and H. J. Weber, *Mathematical Methods for Physicists*. San Diego, CA: Elsevier, 1985.
- [33] W. M. Boerner, W.-L. Yan, A.-Q. Xi, and Y. Yamaguchi, "On the principles of radar polarimetry: The target characteristic polarization state theory of Kennaugh, Huynen's polarization fork concept, and its extension to the partially polarized case," *Proc. IEEE*, vol. 79, no. 10, pp. 1538-1550, Oct. 1991.
- [34] S. R. Cloude, "The characterization of polarization effect in EM scattering," Ph.D. dissertation, Univ. Birmingham, Fac. Eng., Birmingham, U.K., 1986.
- [35] S. R. Cloude and E. Pottier, "Application of the H/A/ α polarimetric decomposition theorem for land classification," *Proc. SPIE*, vol. 3120, pp. 132-143, 1997.
- [36] S. R. Cloude, J. Fortuny, J. M. Lopez, and A. J. Sieber, "Wide band polarimetric radar inversion studies for vegetation layers," *IEEE Trans. Geosci. Remote Sens.*, vol. 37, no. 5, pp. 2430-2441, Sep. 1999.
- [37] E. Krogager, "New decomposition of the radar target scattering matrix," *Electron. Lett.*, vol. 26, no. 18, pp. 1525-1527, Aug. 1990.
- [38] R. Touzi, F. Charbonneau, R. K. Hawkins, and P. W. Vachon, "Ship detection and characterization using polarimetric SAR," *Can. J. Remote Sens.*, vol. 30, no. 3, pp. 552-559, 2004.
- [39] R. M. A. Azzam, *Ellipsometry and Polarized Light*. Amsterdam, The Netherlands: North Holland, 1977.
- [40] R. Touzi, W. M. Boerner, J. S. Lee, and E. Luneburg, "A review of polarimetry in the context of synthetic aperture radar: Concepts and information extraction," *Can. J. Remote Sens.*, vol. 30, no. 3, pp. 380-407, 2004.
- [41] C. Lopez-Martinez, E. Pottier, and S. Cloude, "Statistical assessment of eigenvector based target decomposition theorems in radar polarimetry," *IEEE Trans. Geosci. Remote Sens.*, vol. 43, no. 9, pp. 2058-2074, Sep. 2005.
- [42] R. Touzi, "A unified model for decomposition of coherent and partially coherent target scattering using polarimetric SARs," in *Proc. IGARSS*, Seoul, Korea, 2005, pp. 4844-4847.
- [43] R. Touzi, A. Lopes, J. Bruniquel, and P. W. Vachon, "Coherence estimation for SAR imagery," *IEEE Trans. Geosci. Remote Sens.*, vol. 37, no. 1, pp. 135-149, Jan. 1999.
- [44] R. Touzi, R. Landry, and F. Charbonneau, "Forest type discrimination using calibrated C-band polarimetric SAR data," *Can. J. Remote Sens.*, vol. 30, no. 3, pp. 543-551, 2004.
- [45] R. Touzi, "Speckle effect on polarimetric target scattering decomposition of SAR imagery," *Can. J. Remote Sens.*, vol. 33, no. 1, pp. 543-551, Feb. 2007.



Ridha Touzi (M'93) received the Ing. degree from l'Ecole Nationale de l'Aviation Civile, Toulouse, France, in 1983, the M.S. degree (D.E.A. and M.S. degrees) from l'Ecole Nationale Supérieure de l'Aéronautique et de l'Espace, Toulouse, in 1984, and the Ph.D. degree and le diplôme de l'Habilitation à diriger des recherches from l'Université Paul Sabatier, Toulouse, in 1988 and 1996, respectively.

From 1988 to 1990, he was a Research Scientist with the Centre d'Etude Spatiale des Rayonnements. From 1990 to 1992, he was with the Canada Centre

for Remote Sensing (CCRS), Natural Resources Canada, Ottawa, ON, as a Canadian Government Laboratory Visiting Fellow. From 1992 to 1994, he was a Professor with the Royal Military College of St-Jean, Québec, Canada. In 1994, he joined the CCRS as a Research Scientist. His research interests include many aspects of SAR image processing, polarimetry, and interferometry, and airborne and spaceborne SAR calibration.

Dr. Touzi was a recipient of the 1999 Geoscience and Remote Sensing Transactions Prize Paper Award for his study on the "Coherence Estimation for SAR imagery," and the Natural Resources Canada 2003 Award for his significant contribution to the field of polarimetry in Canada and to Canada's preparation of RADARSAT-2.